Universiteit Utrecht

Opleiding Natuur- en Sterrenkunde

The Use of Diffusion for Modelling the Distribution of Plastic in the Northern Pacific

Bachelor Thesis

Simon Brouwer

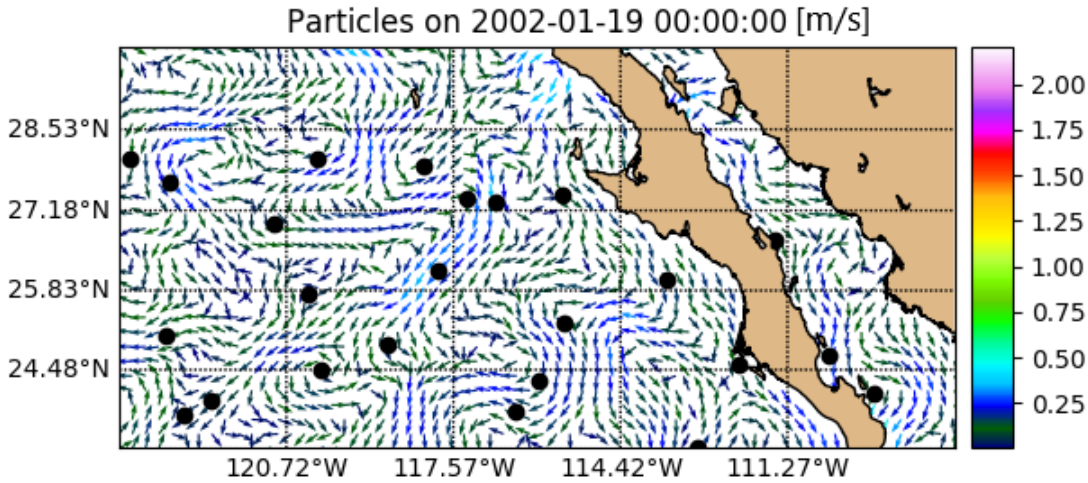

Supervisor:

dr. E. Van Sebille
D. Wichmann

January 17, 2018

Abstract

The problem of plastic in our oceans has received much attention in science and policy in recent years. In this context, Lagrangian particle modelling has been used to better understand the causes behind the plastic accumulation in the subtropical gyres. However, most studies do not take into account the currents which are not resolved by Oceanic General Circulation Models (OGCM) beyond simple linear interpolation.

In this thesis we study to what level of accuracy these sub-grid scale flows can be approximated by three different diffusion models: simple Brownian motion, wind-dependent Brownian motion and the Kinematic Lagrangian Model of Lacorata, Palatella, and Santoleri (2014). We simulate an ensemble of 70,000 particles with the Lagrangian particle tracking program Parcels forced by data from the GlobCurrent OGCM for three and thirteen years, and compare the obtained distributions to the drifter-based results of Maximenko et al. (Sebille et al. 2015; Maximenko, Hafner, and Niiler 2012).

The results showed that Brownian motion provides a better fit with observations than simulations with just the large-scale advection components. It was also shown that the optimal amount of diffusivity needed to be higher for the best fit with the Maximenko result than an experimentally determined diffusivity relationship would prescribe. The 'Kinetic Lagrangian Model' was proven not to provide better results than the base-line test and was, therefore, not seen as conducive to providing a better plastic distribution.

This thesis was concluded by suggesting that further research needed to be done into the oceanic-coastal interface.

The image on the front page is a snap shot of the GlobCurrent at 19 January 2002 in Parcels with some particles visualised near the Gulf of California.

Contents

1. Introduction

One of the great environmental problems of this day and age is the concern for plastic litter in the world's oceans. It is a concern which is not only felt by the academics, but also by the general public. People are continually being made aware by governmental and environmental agencies that the extent of the amount of plastic in the oceans is of concern. Certainly the pictures of plastic-strewn beaches, birds filled with plastic and giant clumps of floating debris are well known. From these examples, and from academic research, it becomes clear that this marine plastic, besides being aesthetically unpleasant, also endangers various forms of marine life through ingestion, absorption into the organism itself or through enabling zoological aliens to enter previously closed-off environments (Derraik 2002). The impact which plastic can have on the human quality of life should not be underestimated either. Plastics have been shown to contain compounds which are hazardous to human health (Halden 2010). There are, therefore, dangers involved in the ingestion of plastic compounds through contaminated marine animals (Rochman et al. 2014).

The amount of plastic in the oceans is an on-going topic of research. Though it is a fact that there are large amounts of different types of plastic in the marine environment, available estimations contain a lot of uncertainty. An estimate for 2014 says that the amount of plastic in the ocean is found in between 93 and 236 Gg (Sebille et al. 2015). Besides a gap in the understanding of the amount of plastic. An estimate concerning the yearly amount of plastic that enters the ocean says that in 2010 between 4.8 to 12.7 Mg of plastic entered the oceans, and that this yearly addition to oceanic pollution will grow by an order of magnitude by 2025 (Jambeck et al. 2015). These studies show that there is a large amount of uncertainty considering the amount and growth of all the plastic in the ocean.

It is clear that there is a need to improve the scientific understanding of plastic in the ocean. This can be done in a variety of ways and in this thesis one route is tried. An important tool for studying the distribution of plastic in the ocean is numerical simulation. Considering the amount of plastic in the ocean and the multitude of health and environmental risks which this problem poses, any improvement made to simulation of plastic flow is a welcome one.

There is, furthermore, an added benefit to trying to improve the accuracy of these models: besides deepening the scientific understanding about how plastics move, such an improvement to model accuracy is invariably also an improvement to the general knowledge concerning the movement of small particles in the ocean. It can be said that an unexpected good side to plastic pollution is that this provides researchers with a tracer particle which is many times more abundantly available in the ocean as compared to other objects of the same size in the ocean. What such an abundant tracer particle then allows us to do, is to judge to what degree advection models with input from a Oceanic General Circulation Model (OGCM) can explain the movements of particles which are much smaller than the grid resolution on which the OGCM is defined.

So besides getting an insight into the way an environmental hazard is moved around, improving the simulation of plastic provides us also with a way to better understand the currents which exist below the grid length of an OGCM.

We can understand from the previous that the finite resolution of OGCM data in space-time as compared to the almost infinitely complex nature of the real ocean is a major bottle neck in

trying to represent a natural system in a model. We need to stress here that particle dynamics not only depend on the velocity field in which they exist, but also upon particle properties, like, density and shape.

We are, however, interested in further exploring manners in which the unresolved currents which live below the grid scale of an OGCM data set, can be represented and the differences between particle are, therefore, ignored within this thesis.

To show that there is a big difference in scale between the data set and particle length scale, we can analyse the length scale properties of the OGCM data set that is used within this thesis. The repository that we use, is version 2.0 of the GlobCurrent which contains geostrophic and Ekman components of the current at 1/4°-spacial and 3-hour temporal resolution*. This 1/4° corresponds to a length of approximately 28 km, whilst the floating oceanic plastic which Sebille et al. (2015) included in their plastic count had a length scale between 0.33 and 200 mm.

Every current that then lives on the length scale that lies somewhere from the particle to the GlobCurrent scale is lost. In this thesis an attempt is made to approximate these localised forces by implementing a general form of diffusion through Brownian motion. This might represents the unresolved currents which are not captured by the GlobCurrent.

The argument that this can be done, is mainly bases on the assumption that the sum of all the currents that exist in between the particle scale and the flow data set scale is sufficiently chaotic. This means that whilst all the currents on the sub-grid scale are structured and in a sense deterministically bound by, e.g., ocean geometry, this whole — by virtue of the shear vastness of its scope, is chaotic. This is the reason for us to see whether this chaos could be represented by the random nature of Brownian motion.

This is why Brownian motion can be used as a diffusion model to approximate these unresolved currents.

However, to what system parameter is the strength of Brownian motion linked? In the later sections covering the theory used in the model, there is a detailed explanation of how Brownian motion is implemented, but it is useful to succinctly cover to what parameter(s) Brownian motion is linked.

The strength of the Brownian motion is determined by the diffusivity of a system. In section 2.1 it is stated that this quality depends primarily on the distance between grid points in the data set that contains the advection fields. This type of Brownian motion we call simple Brownian motion. However, it might be interesting to see if the diffusivity can be linked more thoroughly to a more natural system parameter. We suggest that because wind stress leads to more turbulent mixing which brings about an increase of chaos/complexity in the system, an adjustment must be made to the strength of the Brownian motion. This mixture of Brownian motion with a strength dependence on length scale and wind stress, we call wind-influenced Brownian motion.

In any case, the above two types of diffusion are still built on the effect of Brownian motion. To see if a whole different kind of diffusion model can be used as an approximate, we try a diffusion model which is not based upon Brownian motion. In a paper by Lacorata, Palatella, and Santoleri (2014) a so-called KLM† was introduced wherewith the unresolved parts of motion

*For access to the OGCM data set, see `http://globcurrent.ifremer.fr/`.

†*Kinematic Lagrangian Model*

of tracers in the Mediterranean was modelled. An important difference between the KLM and Brownian motion in general is that the first is a determined but chaotic force, whilst the second is simply random. In any case, the authors found results which would suggest that this type of diffusion would work to add chaos to the system. In this thesis, simulations are run to see how this KLM impacts the distribution of marine-bound plastic.

These are then the different diffusion models which are used as an approximation for the unresolved parts of motion. We will now discuss how these forms of diffusion can be cast into mathematical formalism. This is done in section 2. After that we will explain in section 3.2 what external data sets are used in running the model and how the model is run. Furthermore, we will show how from the model results can be extracted that either support or denounce the diffusion approximation.

2. Theory

In this section we cover the three types of diffusion models which are used within this thesis; simple Brownian motion, wind-influenced Brownian motion and the KLM.

2.1. Brownian Motion

One of the two types of diffusion which we have suggested to replace the unresolved currents was Brownian motion. In section 1 we have covered why Brownian motion could be used. Another statement that was made, was that the strength of Brownian motion, i.e. the diffusivity, is primarily dependent upon the length scale between grid points in the OGCM data set. As a side note the suggestion was made that wind stress could also contribute to the diffusivity. This is a hypothesis which is also being made in the papers by Okubo (1971) and Morales, Elliott, and Lunel (1997).

As the first step we cover what the mathematical description of Brownian motion that is true for both the simple and wind-influenced forms of Brownian motion. The important property of this type of motion is that it is a stochastic process: this means that any description that can be given for this type of motion does not describe for a particle the exact trajectory, but it does describe on a macroscopic scale the statistical properties which are associated with the physical process of Brownian diffusion.

In this thesis use is made of eq. (1) from a paper by Spagnol et al. 2002. This form of an equation describing Brownian motion is exactly what is required in this thesis, since it not only allows for an iterative simulation through time, but it also outputs a displacement which can simply be added on top of the movements caused by the large-scale currents.

$$\begin{pmatrix} x_{\mathrm{bm}} \\ y_{\mathrm{bm}} \end{pmatrix} = \left(\sqrt{\frac{2\Delta t}{r}} \begin{pmatrix} R_1 & 0 \\ 0 & R_2 \end{pmatrix} + \Delta t \begin{pmatrix} \partial_x & 0 \\ 0 & \partial_y \end{pmatrix} \right) \cdot \begin{pmatrix} K_U & 0 \\ 0 & K_V \end{pmatrix} \tag{1}$$

In eq. (1) x_{bm} is the Brownian-caused displacement in the zonal direction and y_{bm} is this displacement in the meridional direction; note that both displacements are in degrees. R_1 and R_2 are uniform random numbers distributed around a zero mean and with a variance equal to r. Within this thesis r is equal to a third. This corresponds to the variance of a uniform number

distribution that pulls a number from the range $[-1, 1]$.* The probability distribution function is given in eq. (2). In this equation n represents a number.

The last two quantities in this equation are Δt which is the time skip in between simulation steps, and K_{U} and K_{V} are the values for the diffusivity in $\mathrm{deg}^2/\mathrm{s}$ for the zonal and meridional direction as functions of longitude and latitude. That there exists a distinction between the zonal U-component and the meridional V-component is because the diffusivity is a quantity which primarily depends on the length scale on which the diffusion happens; and on a globe these length scales are different depending on the cardinal direction along which the length in meters of a degree is measured.

$$p(n) = \begin{cases} \frac{1}{2} & \text{if } |n| \leq 1 \\ 0 & \text{else} \end{cases} \tag{2}$$

In the case of the model which is used in this thesis, the length scale equals the grid spacing for the GlobCurrent, as explained in section 3.3. This spacing equals 1/4°. in both the zonal as the meridional direction. An experimentally determined relationship between the length scale and diffusivity was shown by Okubo 1971 to equal:

$$K_{\mathrm{cgs}} = 0.0103 l^{1.15}, \tag{3}$$

wherein K_{cgs} is the diffusivity in cm^2/s and l is the length scale in cm. Do note carefully that the units used in eq. (1) are different from those in this equation. Special care has to be taken when converting from centimetres to degrees, because the relationship between a length in the zonal direction in centimetres and degrees is $\propto \cos^{-1}(y)$ with y the particle latitude in degrees, whilst the conversion in the meridional direction is position independent.

2.2. Brownian Motion with Wind Influence

With Brownian motion and the definition of the diffusivity in eq. (3). We can run models where we have a combination of OGCM-caused advection and simple Brownian motion; to quickly reference to this type of Brownian motion, we give it the name type-0 or T0 Brownian motion. However, we can modify the definition of the diffusivity to also include a dependency on the wind stress.

To achieve this, one would first need to determine what the coupling between wind and Brownian motion is. A simple starting description would be that this coupling is proportional to the strength of diffusivity as prescribed by eq. (3), and that whilst the maximal wind contribution to the diffusivity should be lesser, the addition of the effect is taken to be quite significant. This is primarily done to clearly study the effect of the wind parameter and is not based on an analysis of the effect or on results from other research.

A follow up enquiry would be how the wind effect would be represented in the addition. It is certainly possible to use a data set containing the surface wind stress over the pacific during the years the model is run, however, in this thesis the wind over the pacific is highly simplified through a series of assumptions.

*Quick proof: $r = \left\langle n^2 \right\rangle - \langle n \rangle^2 = \frac{1}{2}\int_{-1}^{1} n^2 \,\mathrm{d}n - \left(\frac{1}{2}\int_{-1}^{1} n \,\mathrm{d}n\right)^2 = \frac{1}{3}$

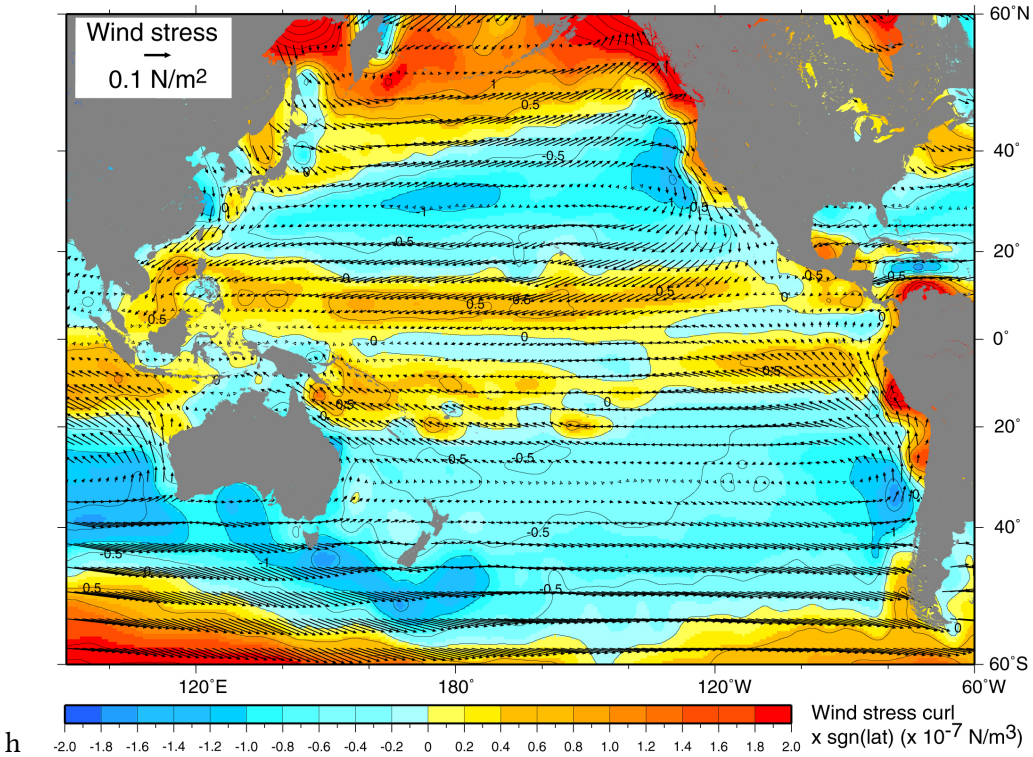

h

Figure 1: Annual mean winds with wind stress (N/m^2) (vectors) and wind-stress curl ($\times 10^{-7}$ N/m^3) (color), multiplied by -1 in the Southern Hemisphere. This image was taken from `http://booksite.elsevier.com/DPO/chapterS10.html` and then slightly modified to not include the subfigure marker.

The first assumption is that we only take into account the trade winds, because these are constant in time for the time span this model is run for. In fig. 1 the winds are shown in the Pacific. If we now focus on the winds in the Northern pacific from 0° to 60° N, it is clear that they are primarily zonally orientated. Furthermore, if one were to describe the form and strength of this zonal component, then you could state as a first, crude approximation that $\tau_x \propto \cos(ky)$, with τ_x the wind stress at the ocean surface, k the wavenumber which is estimated to equal $^{\pi}/_{30}$ deg^{-1} and y is the latitude in degrees.

With these simplifications in mind, further progress can be made in completing the wind-influenced part of the diffusivity. This is not too difficult to do, as it simply consists of multiplying the wind addition with the absolute value of the sine function with which the horizontal wind stress scales. Do take note that the absolute value of the sine is taken here for the addition, and not just the sine. This is done because whilst the wind stress does have a direction, diffusivity does not. The latter, as was stated in the beginning of this section, is proportional to the strength of the wind, and not to its orientation.

$$\begin{pmatrix} K_{\text{U-wind}} \\ K_{\text{V-wind}} \end{pmatrix} = \left(1 + \frac{1}{2}\left|\sin\left(\frac{\pi}{30}y\right)\right|\right)\begin{pmatrix} K_{\text{U}} \\ K_{\text{V}} \end{pmatrix} \tag{4}$$

The diffusivity in eq. (4) can now be used in conjunction with the Brownian motion model given in eq. (1) to run simulations with a combination of OGCM-caused advection and Brownian motion that has a diffusivity which includes parametrised wind; for ease of reference we call this model of Brownian motion type-2 or T2 Brownian motion.

Do note that in eq. (4) we have assumed that an increase in zonal wind stress leads to both an increase in zonal and meridional diffusivity. We assume that this is right because we recognise that what the extra diffusivity replaces, is not the effect of particles being pushed by the wind. What is replaced, are the localised turbulent currents which are determined by the wind strength; and definitely these cause particle motions to become more chaotic, even though trade winds have a habitual orientation. This means that there is reason to increase the diffusivity in both directions.

However, to support the validity of this assumption on the nature of the wind effect, simulations are also done which only make use of a diffusivity contribution in the zonal plane so that these different implementations can be compared. The equation for the diffusivity that is used in these cases is the one in eq. (5). The combination of this diffusivity in the Brownian motion model plus OGCM-based advection we call Brownian motion type-1 or T1.

$$\begin{pmatrix} K_{\text{U-wind}} \\ K_{\text{V-wind}} \end{pmatrix} = \begin{pmatrix} K_{\text{U}} \\ K_{\text{V}} \end{pmatrix} + \frac{1}{2} \left| \sin\left(\frac{\pi}{30} y\right) \right| \begin{pmatrix} K_{\text{U}} \\ 0 \end{pmatrix} \tag{5}$$

As a final check to see if the possible increase in quality of the match between the model and Maximenko results is rooted in the wind approximation and not in the on-average higher diffusivity, a simulation with Brownian motion is run which has a flat 50 per cent increase in overall diffusivity strength. This is to see if the change in fit quality is primarily dependent upon the inclusion of a wind parameter in the system or upon the flat diffusivity increase.

2.3. Brownian Motion Optimisation Analysis

Another aspect of Brownian motion that is interesting to research, is if eq. (3) describes the optimal value for diffusivity to use in this model for a given length scale. It might very well be that a higher or lower diffusivity results in a better fit for the simulation to the Maximenko result. To explore this issue, multiple simulations are run with different diffusivity values.

In the case of this thesis ten models are run with a global diffusivity multiplier which jumps from 0 to 4.5 in steps of 0.5 in between steps. The simulation is also initialised in a slightly different way: instead of starting on an uniform grid with 0.25° longitudinal spacing and 0.4° latitudinal spacing, an interval size 0.5° between grid points in both directions is used. This is mainly so as to cut back on calculation time, whilst keeping the resolution of the model high enough to extract usable results from it. These models are run for both the time span of three and thirteen years.

2.4. Kinematic Lagrangian Model, or KLM

The final type of diffusion which is studied, is one suggested by the researchers in the paper by Lacorata, Palatella, and Santoleri 2014. Herein they used a so-called KLM model to fill in for the turbulent parts of motion which drifters in the Mediterranean Sea underwent. Their model is

predicated upon the idea that the turbulent motion is akin to a summation of differently scaled simplified Rayleigh-Bénard convection cells. The velocity field brought about by the KLM is:

$$\begin{aligned} u_{\mathrm{KLM}}(x,y,t) &= \sum_{n=1}^{N_m} A_n^U \sin\left[k_n^U x - \frac{\pi}{5}\sin\left(\omega_n^U t\right)\right] \\ &\quad \times \cos\left[k_n^U y - \frac{\pi}{5}\sin\left(\omega_n^U t + \theta_n\right)\right] \\ v_{\mathrm{KLM}}(x,y,t) &= -\sum_{n=1}^{N_m} A_n^V \cos\left[k_n^V x - \frac{\pi}{5}\sin\left(\omega_n^V t\right)\right] \\ &\quad \times \sin\left[k_n^V y - \frac{\pi}{5}\sin\left(\omega_n^V t + \theta_n\right)\right] \end{aligned} \tag{6}$$

In eq. (6) A_n^i is the amplitude of motion, k_n^i is the wavenumber whilst ω_n^i is the frequency of the temporal oscillation. In all these cases i denotes the unit direction of the variable, either U or V and n indicates a countable sub-mode in a series of N_m modes that make up the final result. That we denote a difference in the variables depending on which unit direction the variable is taken, is because all these have a dependencies on the length scale. And just as it was with the conversion from a length in centimetres to degrees for eq. (3), the variables in eq. (6) that depend on a length are $\propto \cos^{-1}(y)$ in the zonal direction with y the latitude of the particle whilst this dependency does not exist in the meridional direction.

The next step then would be to find a series of modes which best replaces the unresolved parts of motion. This, however, we have not done, because one would need to do a drifter analysis to map the KLM modes to the seen unexplained movements and this is considered to be outside the scope of this thesis. As an initial try to see if KLM can work as a replacement diffusion model, the modes found by the researchers in the paper by Lacorata, Palatella, and Santoleri (2014) looking at unexplainable drifter motion in the Mediterranean is used.

$$\begin{aligned} l_n^i &= 2^{-1/2} l_{n-1}^i & A_n^i &= \left(\mu l_n^i\right)^{1/3} & k_n^i &= 2\pi / l_n^i \\ \omega_n^i &= \pi A_n^i / l_n^i & \theta_n &= \pi/4 \end{aligned}$$

Herein μ in the equivalent mean turbulence dissipation rate and it equals $10^{-9}\mathrm{m}^2\mathrm{s}^{-3}$. The value of the number of modes (N_m) was set to six in their solution and $l_6^{U,V}$ is equal to 10 km. Again, remember here that in metres $l_6^U = l_6^V$, but in degrees this relation is not true, e.g., for a particle at 30° N $l_6^U = 2.9°$ and $l_6^V = 2.5°$.

To finally apply these fields in the model, they need to be numerically integrated. The scheme we use for this is the classical Runge-Kutta or RK4 scheme.

3. The Model

3.1. Parcels and Model Running

To facilitate the simulation, a program called Parcels* was used. This program allows users to create small kernels which dictate what particles should do. In this thesis we have created a

*The program itself is discussed in Lange and Sebille 2017, furthermore, it is freely avaible on Github at `https://github.com/OceanParcels/parcels`.

basic framework on which all the different kernels are based. This framework consists of three parts: (1) an implementation for zonal periodicity which allows particles to jump between -180° and +180°. (2) A logic check to see if a particle is at a location where it can be advected. This condition is true if a particle is at a location where it has an entry for the current strength; when this is not so, we tag the particle as being beached. (3) The equation of motion which is used to advect non-beached particles during the simulation.

The equations of motions that are used in this thesis are covered in section 2. Here one can see that the equations of motion all consist of an advection and a diffusion implementation, like Type-0 Brownian motion. The advection implementation is done through a RK4 numerical integration of a particle in the OGCM data from the GlobCurrent (see section 3.3). If a particle cannot be directly located on a grid point in the GlobCurrent, then a new velocity is construed through linear interpolation to its nearest neighbours.

We then run such a kernel with equations of motion embedded into it for either three or thirteen years. We go through this temporal domain with time steps of 5 minutes between iterations. After running this loop for fifteen days, the model handles all the particles that have beached; what happens to these is discussed in section 3.1.1. A visual representation of how the kernel is used, is given in fig. 2.

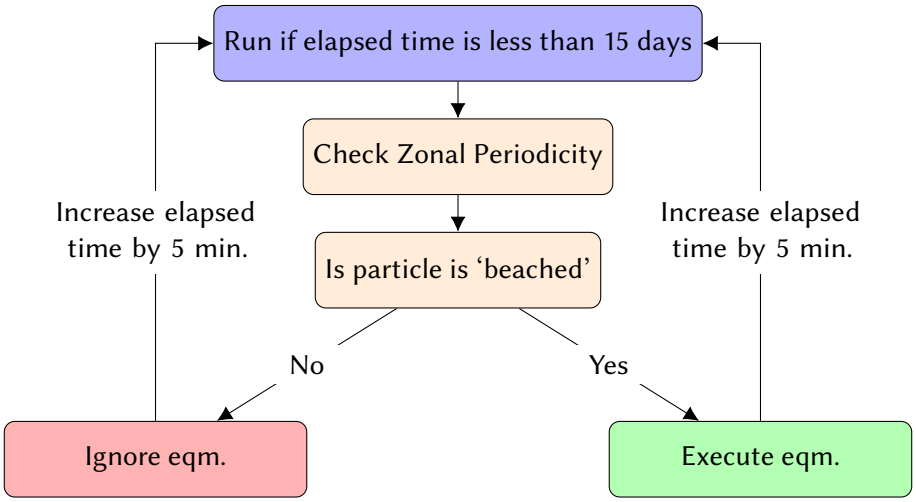

Figure 2: Basic scheme of how a kernel is used within the simulation. As can be seen, to execute the loop 15 days are split up in iterative steps where each one covers 5 minutes. After 15 days are run, the model will handle the particles that are beached.

The initial start of the model has all the particles on a grid with 0.25° spacing in the zonal direction and 0.4° spacing in the meridional direction. This grid itself runs from 65°N and 120°E to 0°N and 100°W; this covers the Northern Pacific and some parts of the Chinese Sea. Of course some of the particles in this block start on land, this is an invalid position and we have removed those that start in such an area. That we have chosen to simulate the development of the plastic distribution in the Northern Pacific, is because this particular area has received a great deal of attention in cataloguing its plastic inventory.

3.1.1. Coastal Interaction

As a last point with Parcels and the model in general, the way beached particles are handled needs to be discussed. Firstly it must be determined when a particle is beached and secondly what should happen after such an occurrence has been detected. It is assumed that a particle is beached when its coordinates point to an undefined value in the GlobCurrent. When this happens a particle will be frozen in place and every fifteenth day the program checks which particles have this state. Those that have are then reinserted on a randomly selected grid point that was pulled from the original collection of particles in the uniform distribution.

The underlying physical argumentation here is that it is assumed that the coastal interaction is too complex to be defined in the constraints of this thesis. So a reasonable first guess would be to state that such a particle has been 'lost'. However, because deleting particles gives a skewered result to favour those whose path did not come close to a coast, there is a need to reinsert particles to keep track off how particles move along these coastal danger zones.

However, doing this causes a certain problem to appear: when a particle is randomly replaced on a grid point, its history is erased. This is problematic, because the object of interest is what the realistic plastic distribution should look like. A particle which has just been placed in the model, can only reflect the real distribution as a product coincidence. What is meant by this, is that by reinserting a beached particle on a grid point, you may inadvertently recreate a plastic distribution that shows more fitness to Maximenko's result than when you left the particle beached.

To account for this, we firstly recognise that a particle that has lived for a longer time in the model has more authority in determining the end distribution than a particle that has lived for a shorter time. We represent this observation by determining for each particle a weight value, as defined in eq. (7), and it shows the weight as a function of 'time the particle has been simulated for without beaching' (t_i) in seconds divided by 'the total time the model was run for' in seconds (either three or thirteen years). The subindex refers to the individual particle in question. In section 4 it will be shown how these weights are used.

$$w_i = \frac{t_i}{\tau} \tag{7}$$

3.2. The Global Inventory of Marine Plastics

In section 1 we have stated that measurements on the amount of oceanic plastic contain a lot of uncertainty. This is problematic, because in this thesis there is a need for a general distribution of oceanic plastic; data in the form of localised measurement are not enough to confidently judge the accuracy of simulations. Luckily, research has been done to construct a global oceanic inventory of the plastics.

The general process of measuring plastic is described by Law et al. (2010) and Law et al. (2014). They describe that in their cases ships towed with a plankton net, i.e. a net with a mesh spacing near 0.3 mm, for a certain length. From the amount of plastic in the net and the distance travelled during the tow, the numerical or weighted density can be determined at .

Doing this measurement is in itself not problematic. What is problematic is to do enough of these measurements to create a plastic inventory for all the world's oceans. For example, in Law

et al. (2014) the area covered by each bin describing the plastic density is 1°×1°, and to achieve this resolution within an area which roughly runs in longitude from Hawaii to the American East Coast and in latitude from the northern tip of Peru to the Gulf of Alaska, 2529 different plankton net tow runs had to be made which were done from October 2001 till December 2012. One can readily understand from this that taking these measurements demands a lot of time and effort.

An added problem is also that not all oceanic regions have received the same attention when it comes to conducting these measurements; the lack of trawl data for plastic near the southern hemisphere is to such a degree that the existence of accumulation zones can scarcely be confirmed there (Sebille et al. 2015). Furthermore, the different organisations which do these tests use differing standards.* This means that when a global inventory of plastic is composed one shall run into issues which come about by trying to combine data sets from different origins.

For example, in a paper by Sebille et al. (2015) it is reported that their combined data set of trawls across the globe used plankton nets which had differing mesh spacings between 0.15 to 0.3 mm, though it ought to be said that 90 per cent of the trawls used a mesh spacing of 0.333 or 0.335 mm. Of greater importance is the fact that the time range in which these data sets were collected runs from 1971 to 2013. This suggests that such an inventory does not give an exact picture of the plastic in the ocean at a definite point in time.

To quickly summarise what is known about the difficulties which are had with composing a global ocean plastic inventory:

- A global inventory of oceanic plastic has such a temporal range that it is difficult to call the inventory a 'snapshot in time' of the actual inventory.
- There is a substantial difference between oceanic regions with their amounts of documentation for plastic content.

Having recognised these two difficulties, the authors of the paper by Sebille et al. (2015) first applied a plastic growth function which was either a smooth term or a first/second order polynomial, because plastic pollution has only increased since its production started. Therefore, this was done to equate the different measurement years with one and another to the same year, namely 2014. Do note, however, that the distribution of plastics on the ocean surface is not wholly dependent on the ocean currents, but it also varies because of forces which are not so temporally invariant as the main ocean currents in the looked-at timespan.

The main force which can cause such variability on the distribution of plastic is the wind force. That is because through vertical mixing at the ocean-atmosphere interface the wind can directly influence how particles get distributed. To account for this fact, the researchers also applied wind data to their equalisation of the temporal element of the plastic inventory snapshot.

To garner a fix for the problem raised by the second bullet point the same researchers used three different oceanic models to simulate the distribution of virtual particles in the oceans. This was done so as to provide data on the distribution of particles where the standardised data set was lacking. To judge the accuracy of the model solution the plastic count density was

*The Sea Education Association (SEA) is one such organisation that has organised such trawls. In the paper by Law et al. (2014) SEA's standards are covered in depth.

calculated for both the solutions as the standardised dataset in 1°×1° bins. These bins were then inter-compared through a spacial regression analysis.

The results which they obtained showed a reasonable fit with the standardised data set, even more so considering the amount of unresolved motions that there are in the system. In this thesis one of these modulation results is used as the *de facto* global inventory for oceanic plastic. The favoured result is the Maximenko model.

The reason for admitting this result as the future basis for the results acquired in this thesis is because the Maximenko model exhibits the most similarities with how the model in this thesis shall be initialised. As will be shown later both the Maximenko model and the diffusion model start with a uniform distribution of the particles (Maximenko, Hafner, and Niiler 2012), whilst the other two solutions in the Sebille paper do not start with a uniform input but with a coastal injection distribution which was based on the population density at coastal regions.

Another important property of the Maximenko result is that the distribution is calculated by utilising a transition matrix which was constructed by Maximenko et al. through analysation of drifter data. The other distributions in Sebille et al. (2015) do not directly implement drifter data in determining their distributions. Seeing as how in this thesis particles are simulated through a combination of OGCM-based advection plus diffusion, the transition matrix approach of Maximenko et al. is closer to how the simulations in this thesis are run.

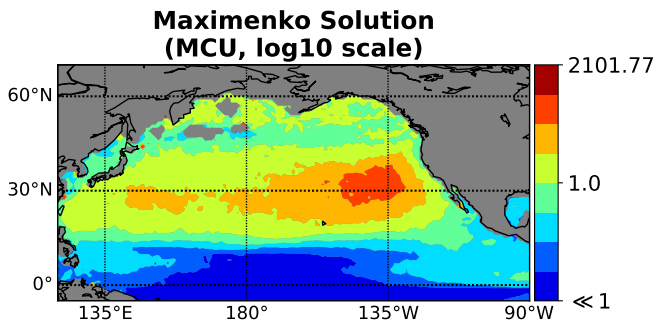

Figure 3: The Maximenko model for the distribution of plastic zoomed in on the Northern Pacific from a world-wide data set which was presented in the Sebille et al. 2015 paper. The 'Mean Cell Unit' (MCU) scale is covered in section 6.

3.3. Model Forcing Data

We said in section 1 that we use the OGCM data from the GlobCurrent project to simulate the advective currents. We have also covered in the same section some of the properties of this OGCM data set, we will now cover in more detail the precise subset of data that is taken.

We use 'version 2.0' of the GlobCurrent* containing the geostrophic and Eckman components of the surface current. This data set provides these current components for all the worlds oceans on a 0.25° by 0.25° grid for all longitudes and latitudes — excluding those latitudes near the Arctic and Antarctic Circle. The temporal range of the data is used from 1 January 2002 to 31rd

*URL link to the GlobCurrent project: `http://www.globcurrent.org/`.

December 2014. Within this thesis models shall be run for three and also thirteen years* both starting on 1 January 2002.

4. Result Analysis

The last topic of discussion concerns how the different diffusion models can be compared to each other and the Maximenko model. To this end there are two different representations of the results in this thesis: one is used to allow for visual inspection of the plastic distribution, and the second one is used to quantify the amount of similarity between distributions.

For this analysis — especially the comparison with the Maximenko model, the individual particles must be binned to allow for an easier way of comparison between different results. What we have defined as a bin is an 1°-by-1° object. We have as many bins as is necessary to fill a 2D space which runs in longitude from 0° to 360° and in latitude from -90° to +90°. This definition of a bin and in which space the collection of bins are placed is the same as was used in the paper by Sebille et al. (2015) for the Maximenko result. The binning process is done by adding the weight value (as was defined in eq. (7)) of each particle to the bin to which a particle's coordinates correspond.

The follow-up step is to divide the weighted sum in each bin by the area in kilometres that the bin covers on the globe. From this we get a weight density for each bin. The reason this is done, is twofold: First, because the area covered by each bin in km^2 is not always equivalent to one and another, you could get a skewered picture about how much plastic there is in a bin, and second, because the Maximenko model is also given in particles per km^2 there exists also a practical reason to do the conversion.

Earlier in this section was said that one of the result representations which was wanted, was a visual plot of the distribution of plastic. With these bins this can be done through plotting the contents of each bin as a contour level on a world map, so that one acquires an easily understood plot of not only the relative density of plastic particles at each position in the Northern Pacific, but also of what the spatial gradients are of the plastic density in this area.

For quantifying the similarities between different results, a spatial regression analysis is done. What this means is that each bin cell from one data set is plotted against the corresponding cell in another set. What one sees in data sets which have a close correspondence to each other, is that the plotted points are on a linear fit described by $y(x) = ax$ with a some constant which is determined by the relative linear scaling difference between two sets. To then quantify the fitness, a correlation coefficient is calculated between this imaginary line $y(x)$ and the points determined by linked cells. Note that this process is only done for the bins which fall in the area covered by the initial uniform particle distribution.

The values of this analysis can be used by themselves to judge quantitatively the quality of a fit. However, one can also compare the correlation coefficients of two analyses with the same equations of motion but with differing model run lengths to judge how fitted a model stays to the Maximenko distribution through time.

A side note on this last analysis must be made with respect to the results which will be obtained from doing what is described in section 2.3. The same analysis as given above is

*The days are counted here inclusively.

done, but instead of looking at each individual analysis, a graph containing each correlation coefficient as a function of the diffusivity at the equator will be plotted.

5. Simulation overview

Before the result are shown, it might be helpful to provide a small diagram covering all the different model configurations which are run. You can see this visualisation in fig. 4.

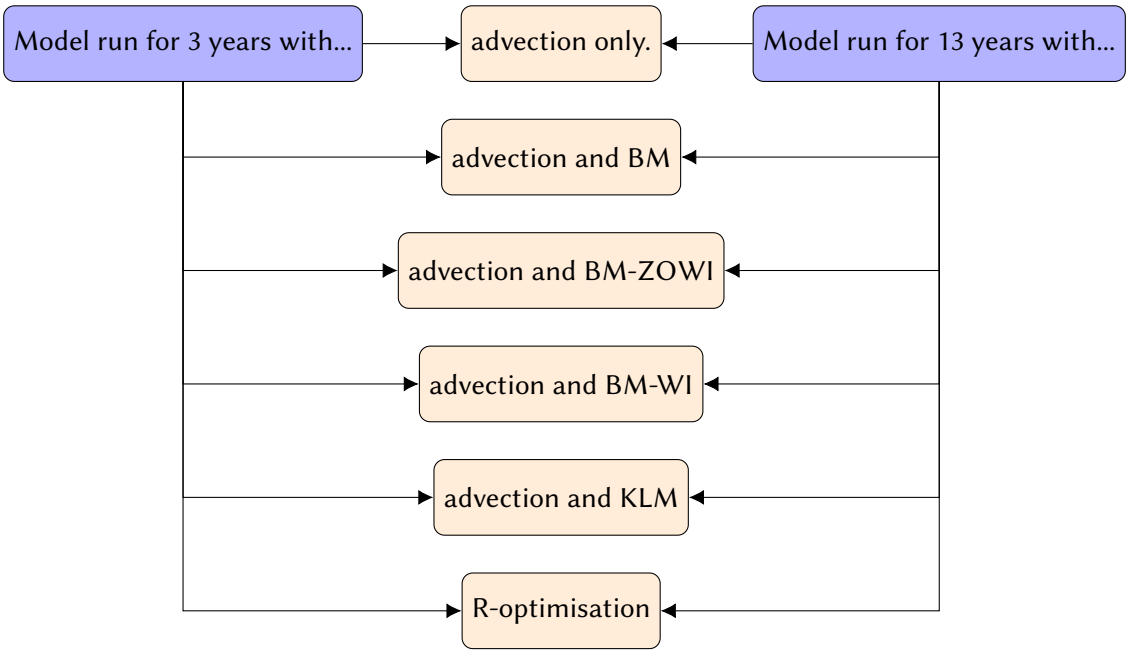

Figure 4: Possible simulation durations with model components. In this figure BM stands for Brownian Motion, see section 2.1, and ZOWI and WI stand for (zonal only) wind influenced whose definitions were covered in section 2.2, and KLM refers to the 'Kinetic Lagrangian Model'. 'Advection' in these blocks refers to the movement caused by the current fields in the GlobCurrent.

6. Results — Density Distribution

After having run the models as is specified in section 3.1, the end distributions are plotted in figs. 5 to 6. In fig. 3 the Maximenko model — as given in the paper by Sebille et al. 2015, is displayed for the same area of interest as of this thesis.

The unit scale used in the plots of the distribution is in 'Mean Cell Units' (MCU). We have defined one MCU as being the mean content of the bins which have a non-zero value for their weighted density. This scale is more useful in determining how convective a distribution of a simulation is than keeping the bin content in #/km^2, because on the MCU scale convergent and divergent behaviour become more apparent in higher and lower extrema.

As can be seen in fig. 5a the particles have a tendency to converge from all latitudes towards 30°N, furthermore, a similar effect also seems to happen in the zonal direction. As can be seen when plot (a) is compared to (b), there happens to be also a tendency to pull particles towards 135°W. However, note that we do not observe the same convergence in the zonal direction as we have seen in the meridional direction. Another observation is that the advection-only simulation does not predict that there is a heightened concentration of particles near the 60°N band which the Maximenko solution prescribes to be there. This behaviour which we observe in the control set also mirrors plastic distribution results of another Lagrangian particle simulations of plastic by Lebreton, Greer, and Borrero (2012).

Another metric of the control set is the average number of times every particle was beached; for the result in (a) this value is 2.28 $\#^{-1}$ and for (b) this increased to 14.7 $\#^{-1}$. This was determined for a set wherein a total of 70 k# particles where uniformly distributed.

The set of simulations with Brownian motion in fig. 5b shows an increased vertical structure if one compares them to the results in fig. 5a. In the left side of the figure you can see, e.g., that the left tail of the big garbage patch at 30°N 135°W is far more vertically spread out. This structure seems to persist even when the model is run for a longer duration.

A curious observation is that there is still no development of a separate garbage patch at the west end of the tail which was seen in fig. 3. Also worth pointing out is that the big plastic gyre seems to have rotated slightly anticlockwise as compared to both the advection-only set and Maximenko model. What does appear to happen is that the maximum cell density seems to decrease when you compare the results for three and thirteen years of all the Brownian motion sets with the control set.

The differences between the types of Brownian motion, i.e., what the extra diffusivity due to trade winds causes, is not that visible. You do see that the maximum mean cell density decreases and that there is a bit more plastic near the coast of Alaska, but beyond that there are no visible effects.

The final observation is that the average number of times every particle beached in the three year runs were from T0 to T2: 2.15 $\#^{-1}$, 2.24 $\#^{-1}$, and 2.29 $\#^{-1}$. For the thirteen year runs 10.3 $\#^{-1}$, 11.3 $\#^{-1}$ and 11.8 $\#^{-1}$ beach events per particle were counted. The total number of particles in the simulation was the same as in the advection-only run.

The combination of the KLM with GlobCurrent advection, as displayed in fig. 6, shows the most variances when compared to the Maximenko model and the advection-only simulation. The structure is not only far less spread out than in the control and Maximenko cases, but it also seems to be spotted and far more convective than the others.

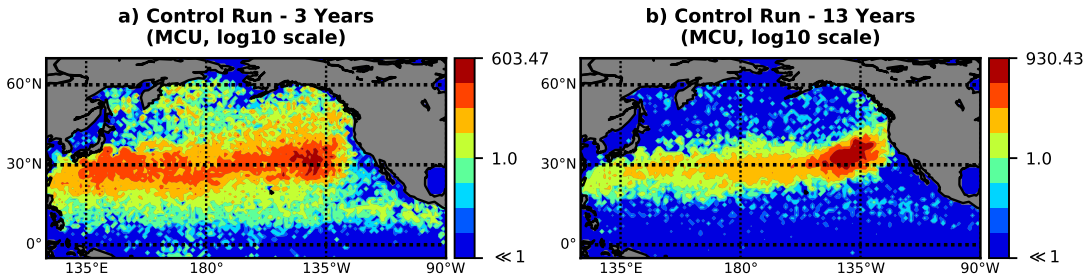

(a) The results of the simulation of virtual particles that are only being forced by the advective currents provided by the GlobCurrent. In subfigure a) the final distribution after three years of simulation is plotted and in plot b) the same equation of motion was used in the Parcels kernel, but the run time of the model is set to thirteen years.

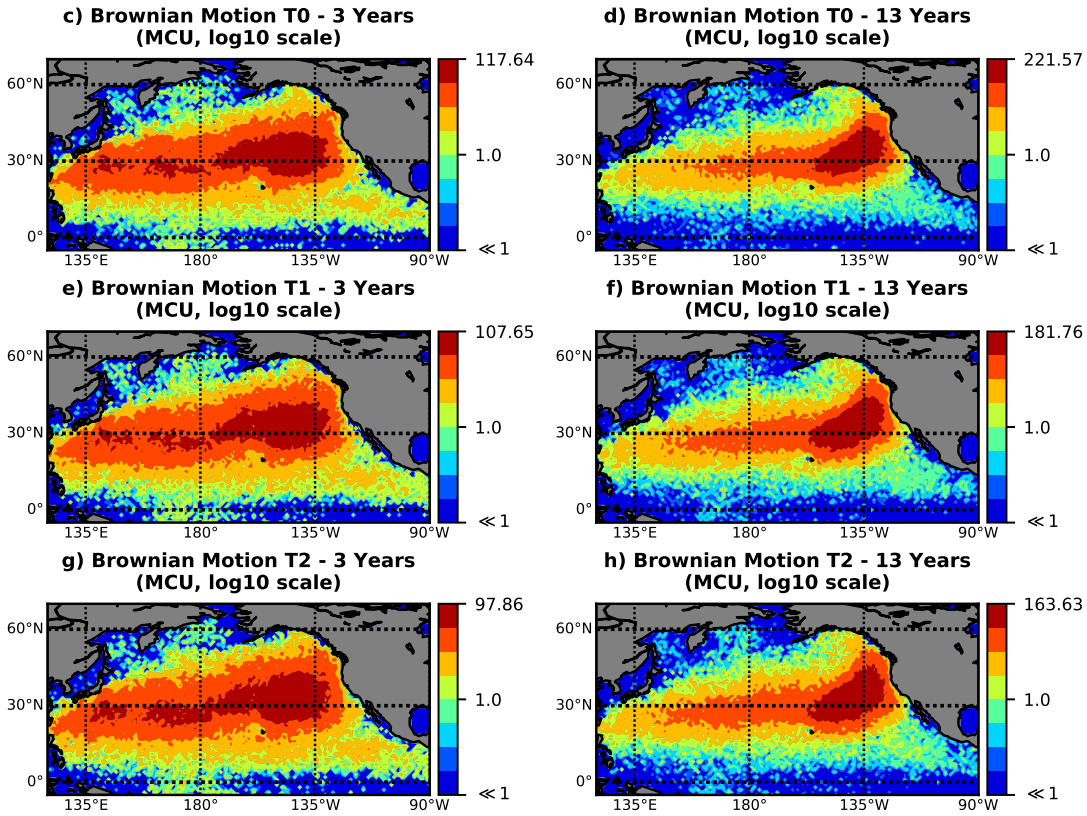

(b) The assorted collection of different types of Brownian motion plus GlobCurrent advection. On the left side of the image the results are given for the end distribution after three years of simulation, on the right this is done for thirteen years of simulation. The first row contains T0 Brownian motion. The second row contains the results with T1 Brownian motion and the third row are the results which used T2 Brownian motion.

Figure 5

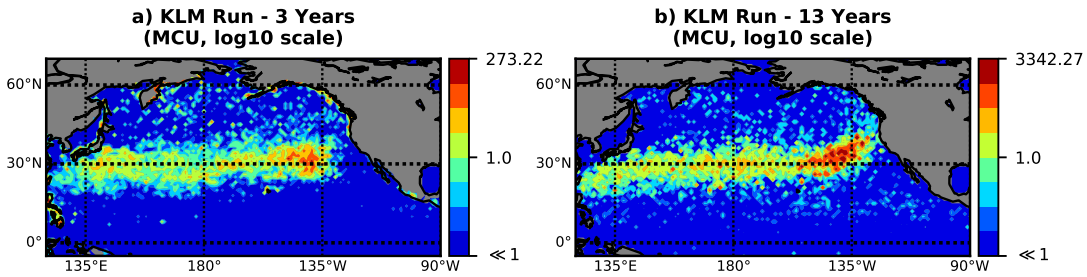

Figure 6: The result of the KLM plus advection simulation. In figure (a) this model was run for three years and in plot (b) you can see the result after thirteen years of simulation.

Another observation is that the highest cell density is many times higher than the average non-zero density cell content. If you compare the KLM maximal cell density after thirteen years with control set after that time, then you can see that the densest cells contained within the KLM is about four times more the average cell content than was seen in the control set. The number of times every particle beached on average, was 5.06 $\#^{-1}$ after three years of simulation and 12.5 $\#^{-1}$ after thirteen years.

7. Results — Regression Analysis

The collection of results for the regression analysis of the models with the Maximenko model are shown in figs. 7 to 10. These results show all the same pattern, though there are some important differences. In all the figures there are quite a few instances where the simulation says there ought to be no plastic particles, whilst Maximenko says there should be. This undershooting by the simulation continues from the left side of each figure till the black 'one-to-one' line; which is an observation which was also made in the previous section where the distribution results were visually inspected.

However, the right side of each figure also shows some interesting results: whilst certainly the model has an tendency to undershoot, it is not to the degree with which it overshoots. As can be seen in, e.g., fig. 7 there are a few outliers on the right-hand side of the figures. Again, this is something which was also noted in the visual inspection of fig. 5a in that the simulation tends to convect particles into the high density patch near 30°N and 135°W.

This observed pattern propagates also through time and has become more extreme after having been simulated for thirteen years. Especially the tendency for the model to undershoot has been increased in fig. 7 at the later date where the thicker part of the correlation plot has shrunk on itself. This increased discrepancy is reflected in the lowering of the correlation coefficient.

In fig. 8 the same trends that were explained earlier can be seen, however, a difference can be seen in that through time the extremity of the model undershoot and the amount in which the model diverges from the Maximenko model also decreases. The latter can be primarily seen by noting that the undershooting does not as substantially increase with respect to what happens in fig. 7. What does clearly increase in the set of Brownian motion simulations, is the strength

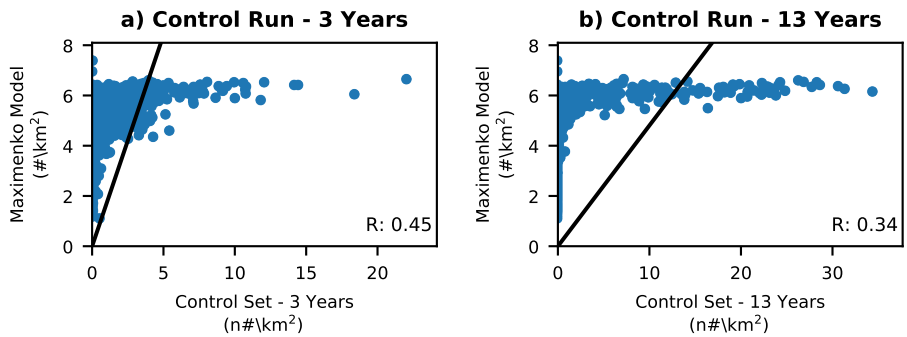

Figure 7: The regression analysis of both the three year and thirteen advection-only simulations against the Maximenko model. A point has as its x coordinate the plastic density for a cell in a simulation result and the y coordinate is the density for the matching cell in the Maximenko result. Points on the black line are where the simulation and the Maximenko data have an one-on-one match for a cell. The R-value in the lower right corner of each figure represents the Pearson correlation coefficient.

of the density overshooting.

As was discussed at the end of section 2.2 an analysis also needs to be done into whether any positive change in Brownian motion with a wind influence approximation is rooted in the fact that the approximation works or that a flat increase of diffusivity would also work. As can be seen in fig. 9 the correlation coefficient does seem to increase over the results in eq. (4). The decrease in correlation is in this case equal to 11.3 per cent.

With the KLM simulation the remark was already made that it looked akin to a spotted distribution with a very high gradient in cell content near the convection zone. In fig. 10 this observation can also be made: as can be seen, there are a few cells which get to accumulate the majority of the particles in the simulation. One also sees that the convective tendencies of this model are greater than those in the control set, because of the very fact that these few cells gain the majority content.

7.1. Regression Analysis with Brownian Motion Optimisation

In fig. 11 one sees the results of different diffusivity values which are greater than what eq. (3) prescribes for the equator. As can be seen by comparing the analysis after three years with the one after thirteen years, there are some noteworthy differences between the right tails of the analyses. But in both cases the strength of the diffusivity which provides the best fit with the Maximenko analysis, is not the value that is described by Okubo's formula.

The analysis after three years shows that the optimal diffusivity value lies somewhere in between 200 and 300 m^2/s for the diffusivity. After this optimum, the regression analysis makes a sharp jump before it settles into a linear-looking decrease of fitness. Another observation that can be taken from this analysis is that even adding a little amount of Brownian motion to the simulation increases the fitness substantially.

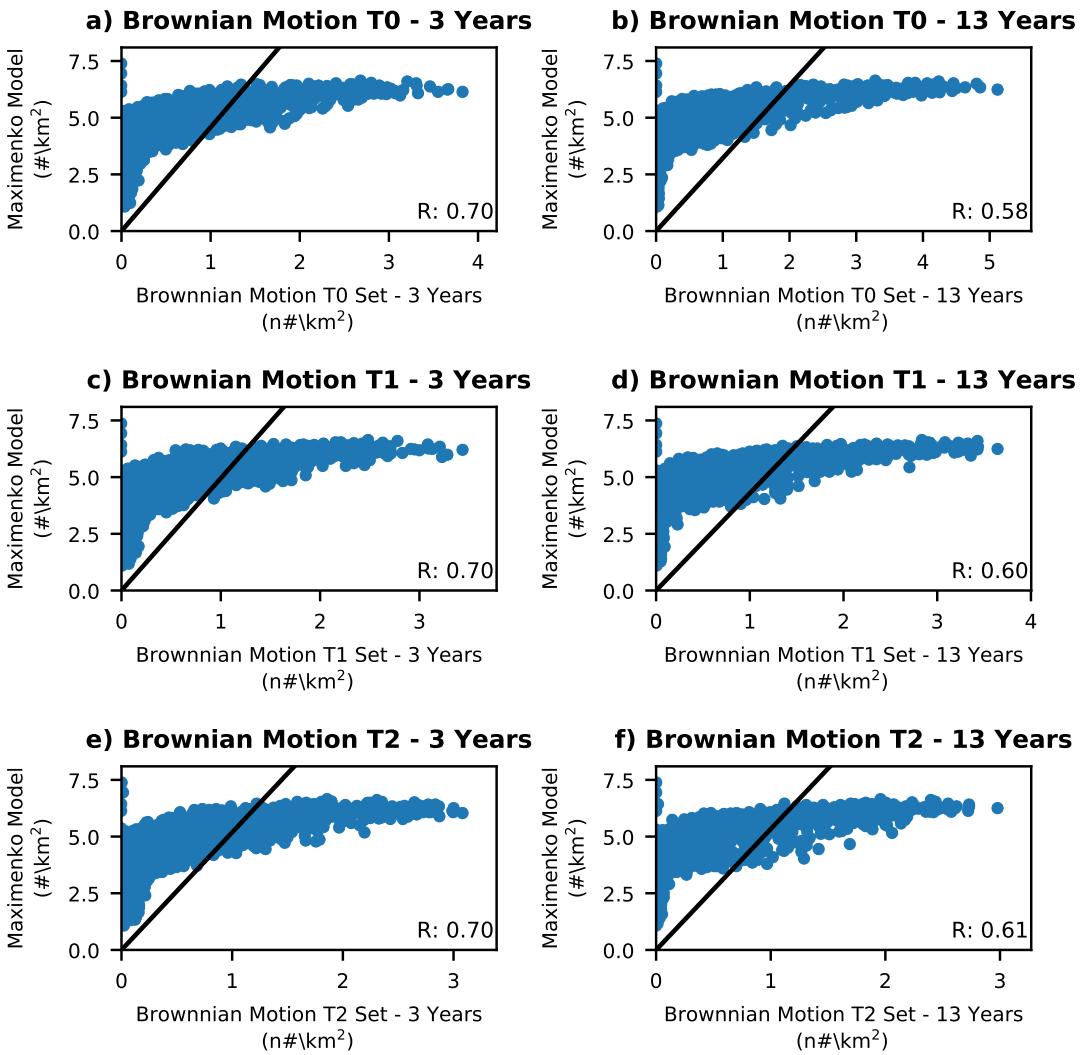

Figure 8: The regression analysis of the collection of different Brownian motion models. The first column contains the results for three years of model run time and the second column for thirteen years of this. From the top row to the lowest the types of Brownian motion used were 'standard', 'extra zonal diffusivity due to wind approximation', 'extra diffusivity due to wind stress at surface'. For an explanation of the black line and the R-value in each plot, see fig. 7.

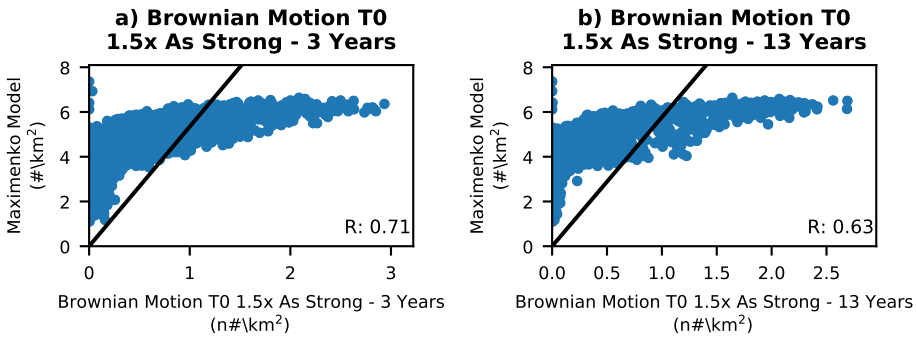

Figure 9: Herein is shown the regression analysis of plastic particles in Brownian Motion plus advection model where the diffusivity used is 1.5 times greater everywhere than eq. (3) prescribes. In these simulations about 30 k# and 48 k# particles were marked as being out-of-bounds for the three and thirteen year run respectively.

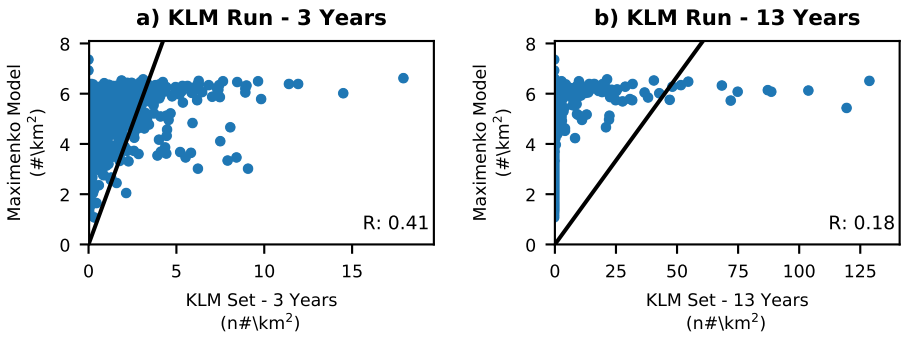

Figure 10: The regression analysis of the KLM. For a definition of the plot parts, see fig. 7.

However, the thirteen year analysis neither shows the same optimal value for the diffusivity nor the sharp jump to the continuously linear decreasing regimen. The optimal value is in this case near 320 m^2/s.

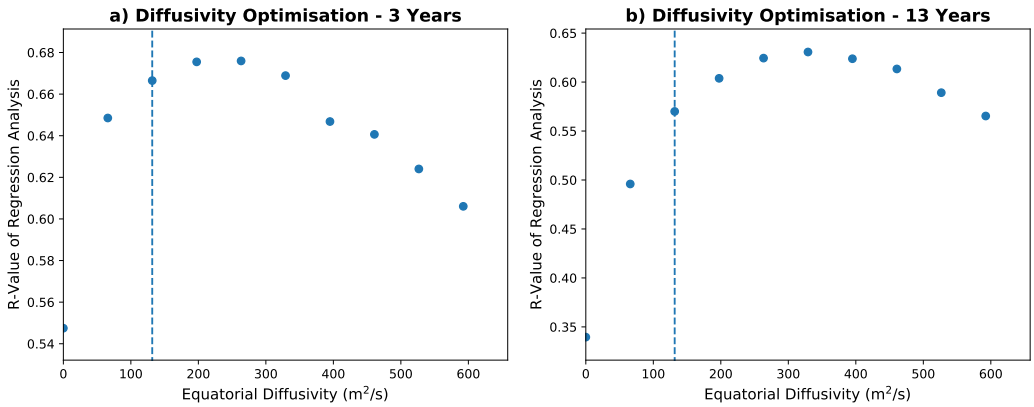

Figure 11: Optimisation of the diffusivity through determining the regression analyses of model cell contents with those in the Maximenko model. The dashed blue line represents the diffusivity which Okubo prescribes for the length scale that fits to 0.25°×0.25° GlobCurrent bins on the equator.

8. Conclusions

It is a certain observation that advection alone cannot explain the distribution of plastic in the Northern Pacific; by way of visual examination of fig. 5a it was noted that the plastic patch expressed a tendency to be completely confined in the Northern Pacific gyre, and mainly in the convergence zone west of California. To express numerically how the inclination to converge creates a growing mismatch between the observed and simulated plastic content, the development of the Pearson coefficients can be examined. In table 1 the R-value went from 0.45 to 0.34; this is 24.4 per cent relative decrease in fitness over 10 years. These values shall be used as a baseline for judging whether a diffusion model improves upon the default fitness or not.

Simulation Set	R-Value after 3 Years	R-Value after 13 Years	Percentile Decrease between Years
Control	0.45	0.34	24.4
Brownian T0	0.70	0.58	17.1
Brownian T1	0.70	0.60	14.3
Brownian T2	0.70	0.61	12.9
Brownian Amplified	0.71	0.63	11.3
KLM	0.41	0.18	56

Table 1: In this table shows the collected correlation coefficients from the figs. 7 to 10. We have also calculated what the percentile decrease was of a set between three and thirteen years of simulation; this is shown in the right most column.

8.1. Brownian Motion

The first type of Brownian motion (T0) showed on visual inspection a better fit with observations. Its R-value through time went from 0.70 to 0.58 which is a 17.1 per cent decrease in fitness. In the case of T1 the R-value goes from 0.70 to 0.60 which indicates a 14.3 per cent decrease in fitness. For the last Brownian motion type, T2, a R-value change from 0.70 to 0.61 was reported; this equates to a 12.9 per cent decrease in fitness. This shows that all the types of Brownian motion not only have a better fit to observations, but also keep through time a better fit.

This validates the hypothesis that Brownian motion could be used to approximate the turbulent currents in the ocean. However, do the improvements to the fitness in the case of the wind approximation come about through it better matching the underlying physics, or does the formula of Okubo* for the diffusivity underestimate the chaotic motion in the ocean — or at least, in the Northern Pacific?

To determine which is the case, a plain Brownian simulation was run wherein the diffusivity was equal to its maximum in those where wind stress was used as a modifier to this amount. The results are given in fig. 9, but the important thing here is that the R-value went from 0.71 to 0.63 which translates to an 11.3 per cent decrease in fitness; which is an result which fits the

*See eq. (3).

Maximenko distribution even better than was found with the T2 Brownian motion. Hence the deduction can be made that wind stress causing extra diffusivity cannot be directly backed up by the results: because a simple multiplication of the the whole diffusivity gives better results than those cases were the multiplication was linked to the zonal wind strength.

A further point of interest in this discussion of Brownian motion concerns the handling of particles which the simulation has designated as being 'out-of-bounds'. As was remarked earlier, these particles that have this event happening to them get reinserted. It was also noted that on average a particle in the control run has more than two collisions with the coast in three years and this number increases to about 15 after thirteen years of simulation. In the case with Brownian motion these numbers overall decrease, but still the average number of collisions per particle is large to such a degree that the correct handling of these events is not a trivial matter.

The action that was defined for handling these events was in this thesis to reinsert a particle at random grid point of the initial distribution whilst keeping track of their 'weighted history length' to make a distinction between younger and older particles. This process was described more in depth in section 3.1, however, this was not the only coastal interaction model that was tried. In appendix A there is a discussion about the different models that were tried and also some suggestions are offered to the problems that will now be covered.

The fundamental assumption that we had made with respect to what the behaviour of particles is near the coast, is that this is unknown. This is of course a crude statement and neglects an important part of the dynamics which ultimately determines the plastic distribution in the ocean: particles near the coast do not simply exit the system.

Whilst it has been shown that Brownian motion can better the results of plastic simulation in the Northern Pacific, it is strongly suggested from the observations made concerning the frequency of coastal collisions of the average particle that in-depth study needs to be done in how-to accurately model the ocean-coast interface. The importance of this problem in the Northern Pacific is in part amplified by the fact that there are a few major currents which are directed along the coast, i.e., the Alaskan, California and Kuroshio current. This causes more coastal collisions to happen than there would be in, e.g., the Southern Pacific, but the importance of coastal modelling is despite of this stressed.

8.2. Brownian Motion R-Optimisation

To study how the fitness of the model was dependent on the strength of the diffusivity in the system, two analyses were done of the different correlation coefficients of models with varying diffusivity. In fig. 11 you can see that the addition of some Brownian motion causes a substantial increase in fitness when compared to the no-diffusivity situation. What is more, the optimal value for the diffusivity is higher than Okubo says it ought to be in both cases; which is a strong suggestion that the diffuse motion in the Northern Pacific, and perhaps other oceans, is greater than Okubo inferred from his experiments where he analysed the diffusion of a fluorescent dye patch through time in different oceanic regions (Okubo 1971).

In section 7.1 it was explained that the different time spans also had a differing optimum for their diffusivity. This is somewhat of a conundrum, because it would provide a clearer and less interpretation dependent result for the implementation of Brownian motion in oceanic particle simulations. One could say that the noticeable shift in where the optimum lies, is an indication

that the analysis does not show where the optimum might be and that in extremis the statement that the diffusivity must be higher for an optimal fit, might be incorrect.

However, it can be argued that the simulation has not yet stabilised after a mere three years of run time and that only at a longer time scale the real relationship between diffusivity and fitness becomes clear. If one takes a look and compares a set of Brownian motion runs in fig. 5b, one clearly sees that the a three-year-run is generally a lot more diffuse than the thirteen-year-run. And this is important, for it can be argued that after three years the simulation has not progressed far enough from its initial uniform distribution. Of course, the system after thirteen years does not have to be the stable state, but the lack of jumps in the correlation coefficients after the optimum at least indicate tentatively a greater amount of stability. In appendix B there is a more in-depth look at the development of this optimisation through time.

8.3. KLM

The KLM simulation provided the most differing result from what the Maximenko distribution claimed it ought to be. The simulation can only with some difficulty be compared to the actual model: the reported R-value in table 1 are not only lower for the KLM than for the control set, but the overal decrease between three and thirteen years is for KLM also higher.

This shows that the KLM model is not a valid replacement approximation for the turbulent currents, because the absolute fitness per snapshot and the relative fitness between years are lower than the results in the control set. However, this makes one wonder why in the paper by Lacorata, Palatella, and Santoleri 2014 the KLM model could be used successfully to simulate drifter motion in the Mediterranean.

A possible answer could be that the Mediterranean has far fewer strong currents, whilst the Northern Pacific contains multiple gyres and strong circulatory currents encircling the Northern Pacific ocean. This is a significant change in the character of the ocean, and it very well might be that the current KLM implementation only works for waters that have no overly strong transport currents.

9. Summary

In this thesis it was shown that Brownian motion could be used as a stand-in for the unresolved parts of motion. However, it was also noted the ocean-land interaction is as of yet an unresolved problem in all simulation set-ups. A suggestion for further research into the viability of this diffusion approximation would in part depend on finding better tools to handle particles near this interface.

Within this thesis attempts were made to link the strength of the diffusivity to the positive impact wind stress has on the strength of turbulent motion at the ocean's surface. It was shown that this relation could not be clearly seen in the results and that a flat-out increase in diffusivity leads to better results than when such increases are linked to the wind stress. However, Brownian motion can be recommended for modellers of plastic, and other oceanic particles, to be included in their simulations, because it counterbalances the too strong convective currents which are encapsulated in the large scale flow.

The results from the optimisation of the diffusivity in the case of non-wind-influenced Brownian Motion show that the equation in eq. (3) underestimates the strength of diffuse effects by a factor in between 1.5 and 2.5. This was seen as a clear indication that the diffuse tendencies of the oceans are stronger than what prior research would indicate.

Simulations with the KLM model showed no improvements over the ones with Brownian motion or even those with only advection. The observations were that the fitness of the distribution quite sharply decreased due to the effects of the KLM. We can, therefore, not yet recommend KLM as an approximation for the unresolved parts of motion. We would like to stress here the fundamental limited scope of a bachelor thesis cannot be used in determining whether a tool developed by a professional research group fails to approximate the unresolved parts of tracer motion; we merely state that within this thesis it could not be used to improve upon the control set.

A. Problems with Boundaries

As was discussed and pointed out in the discussion that was had in the conclusion, the boundaries of the model play a large part in determining how the model develops. This was inferred from the simple fact that every particle had on average 2.28 coastal collision events in three years and 14.7 such events in thirteen years. After diagnosing this, the suggestion was made that serious research had to be done into accurate modelling of what happens at the coast because the used interaction model was probably too simple to be representative of the underlying physical reality.

However, whilst the goal of this thesis was not to really further our understanding of coastal interaction modelling, different attempts were made to find some kind of interaction model which would work with the presupposition that the thesis should not be overly concerned with what happens at the coast; only that what does happen, is something which is not encapsulated into the 'normal' dynamics of the flow in open waters.

The first assumption that was made in all the work on the coastal interaction in this thesis, was that when such an event occurs, the particle becomes an unknown as far as the simulation is concerned. The naive conclusion that one might draw from this is that the particle can simply be deleted. This would be a problematic assumption, because the larger part of particles in the simulation undergo a collision event. If one then were to delete these particles, the picture you would get from doing this would be skewered to preferentially keep the particles in the simulation that were not near the coast.

So this simple idea of removing particles was rejected; ideally the number of particles during the simulation is kept at the same number as when the simulation started. However, in this case a decision has to be made about what happens with a particle that crosses a boundary. In this model what happens at the boundary is a virtual unknown. One interaction choice could be that particles do not really beach, but get stuck a few hundred metres off the coast and to the degree that particles get into this region, they also flow back out into the open ocean.

However, and we have tried this in the model, reinserting particles in the model within a circle area spanned by a radius determined by the maximum standard deviation of Brownian motion, causes hyper particle convergence in certain coastal regions. This is because a particle does not randomly collide with the coast: they are mainly pushed unto the coast because the GlobCurrent advected them thereto. This means that one starts to see particles continually being convected into a coastal area and then getting themselves stuck there, because this interaction mechanic does not push them out of the current which caused them to beach in the first place.

A possible fix to this problem would then be to define a current which is perpendicular to the area where there exists no definition of the GlobCurrent. This makes it less likely that coastal regions become hyper convective zones, but this by itself also causes the occurrence of such zones.

To explain this; imagine that you have an undefined region for the GlobCurrent. Now besides this undefined region there exists a small sliver of cells which do have a GlobCurrent defined and then again some region where there is no current. This means that particles can flow in between these regions. If one then uses perpendicular currents to push particles away from the coast, one may get the situation where particles get trapped within these straits. This causes the problem of hyper convection to again rear its head.

This problem might be solved by padding the undefined grid cells in the current files and then determining the off-shore currents by means of this padded grid cell map. This leads these small problematic edges and small islands to become smoothed out. However, this was not further researched in this paper and this might be the next logical step for other researchers to explore.

As it stands, the most feasible definition of coastal interaction was given in section 3.1.1. Where a particle is reinserted on an original grid initialisation point when is has collided with the coast.

B. Development of the Diffusivity Optimisation

You can see in fig. 12 that the relationship between diffusivity and the correlation coefficient of the model with the Maximenko result becomes a smoother curve after it has been run for more years. However, the mean value of the coefficients does not seem to decrease continuously. What is rather seen, is that the curve oscillates between the years. It is difficult to judge whether this is an effect caused by uncertainties/constraints within the model, e.g., the reinsertion after a out-of-bounds event for a particle, or is it because Brownian motion is an approximation of more complex flow structures? This is an important question, but one which is outside of the scope of this thesis. That being said, it still can be recognised that the shape of diffusivity-'correlation coefficient' relationship retains a high amount similarity between model run lengths; which shows that the optimal value for the diffusivity in the Northern Pacific ought to be higher than what Okubo suggests.

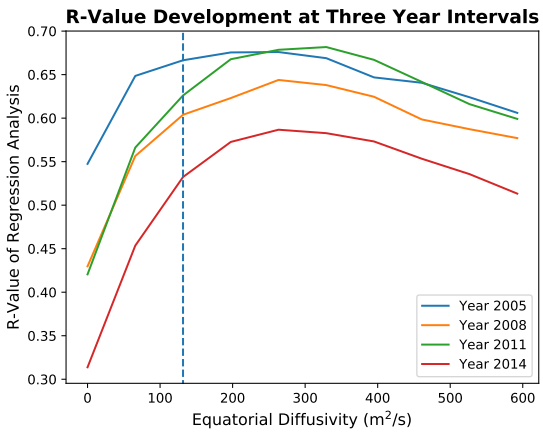

Figure 12: The different curves showing how the correlation coefficients as a function of diffusivity change between different run lengths of the simulation. The starting date for each run was 1 January 2002. The dotted line is the prescribed value for the diffusivity by Okubo for the length scale of a cell in the GlobCurrent which lies on the equator.

References

Derraik, José G.B. (2002). "The pollution of the marine environment by plastic debris: a review". In: *Marine Pollution Bulletin* 44, pp. 842–852.

Halden, Rolf U. (2010). "Plastics and Health Risks". In: *Annual Review of Public Health* 31.1, pp. 179–194. DOI: 10.1146/annurev.publhealth.012809.103714.

Jambeck, J. R. et al. (2015). "Plastic waste inputs from land into the ocean". In: *Science* 347.6223, pp. 768–771. DOI: 10.1126/science.1260352.

Lacorata, Guglielmo, Luigi Palatella, and Rosalia Santoleri (2014). "Lagrangian predictability characteristics of an Ocean Model". In: *Journal of Geophysical Research: Oceans* 119.11, pp. 8029–8038. DOI: 10.1002/2014jc010313.

Lange, Michael and Erik van Sebille (2017). "Parcels v0.9: prototyping a Lagrangian ocean analysis framework for the petascale age". In: *Geoscientific Model Development* 10.11, pp. 4175–4186. DOI: 10.5194/gmd-10-4175-2017.

Law, K. L. et al. (2010). "Plastic Accumulation in the North Atlantic Subtropical Gyre". In: *Science* 329.5996, pp. 1185–1188. DOI: 10.1126/science.1192321.

Law, Kara Lavender et al. (2014). "Distribution of Surface Plastic Debris in the Eastern Pacific Ocean from an 11-Year Data Set". In: *Environmental Science & Technology* 48.9, pp. 4732–4738. DOI: 10.1021/es4053076.

Lebreton, L.C.-M., S.D. Greer, and J.C. Borrero (2012). "Numerical modelling of floating debris in the world's oceans". In: *Marine Pollution Bulletin* 64.3, pp. 653–661. DOI: 10.1016/j.marpolbul.2011.10.027.

Maximenko, Nikolai, Jan Hafner, and Peter Niiler (2012). "Pathways of marine debris derived from trajectories of Lagrangian drifters". In: *Marine Pollution Bulletin* 65.1-3, pp. 51–62. DOI: 10.1016/j.marpolbul.2011.04.016.

Morales, R.A., A.J. Elliott, and T. Lunel (1997). "The influence of tidal currents and wind on mixing in the surface layers of the sea". In: *Marine Pollution Bulletin* 34.1, pp. 15–25. DOI: 10.1016/s0025-326x(96)00058-6.

Okubo, Akira (1971). "Oceanic diffusion diagrams". In: *Deep-Sea Research* 18, pp. 789–802.

Rochman, Chelsea M. et al. (2014). "Polybrominated diphenyl ethers (PBDEs) in fish tissue may be an indicator of plastic contamination in marine habitats". In: *Science of The Total Environment* 476-477, pp. 622–633. DOI: 10.1016/j.scitotenv.2014.01.058.

Sebille, Erik van et al. (2015). "A global inventory of small floating plastic debris". In: *Environmental Research Letters* 10.12, p. 124006. DOI: 10.1088/1748-9326/10/12/124006.

Spagnol, Simon et al. (Jan. 2002). "An error frequently made in the evaluation of advective transport in two-dimensional Lagrangian models of advection-diffusion in coral reef waters". In: *Marine Ecology Progress Series* 235, pp. –.